JOURNAL OF MATERIALS SCIENCE 26 (1991) 510–516

Preparation and characterization of quenched $KNbO_3$–Nb_2O_5 glass

T. SATO, Y. KOIKE, T. ENDO, M. SHIMADA
Department of Molecular Chemistry and Engineering, Faculty of Engineering, Tohoku University, Sendai 980, Japan

$KNbO_3$–Nb_2O_5 glasses were prepared with molar ratio of K/(K + Nb) from 0.16 to 0.5 by using a twin-roller quenching apparatus. Most $KNbO_3$–Nb_2O_5 glasses crystallized to stable phases such as $KNbO_3$, $K_2Nb_4O_{11}$, $K_3Nb_7O_{19}$, KNb_3O_8 and $K_2Nb_8O_{21}$ via metastable phases after heat treatment and $K_4Nb_6O_{17}$ glass directly crystallized to $K_4Nb_6O_{17}$ crystal. $KNbO_3$ glass consisted of the corner-shared NbO_6 octahedra, while the amounts of the edge-shared NbO_6 octahedra in the $KNbO_3$–Nb_2O_5 glass structure increased with decreasing K^+ ion content. The band gap energies and the ionic conductivity of the $KNbO_3$–Nb_2O_5 glasses increased with increasing K^+ ion content, but the density and the activation energy of the ionic conduction decreased. The glasses possessed high dielectric constants approaching those of ferroelectric crystals at high temperature around the crystallization temperature. The dielectric constants of the glasses, however decreased greatly with decreasing temperature and with increasing frequency.

1. Introduction

Since amorphous materials sometimes showed excellent properties such as high permeability, large ionic conductivity, high chemical stability and high fracture strength, many studies have focused on the characterization of amorphous materials. In fact, amorphous materials have been widely used in the fields such as semiconductors and magnets. Recently oxide glasses have attracted much attention, because several quenching techniques which enabled glass materials to be produced containing no network former, have been developed and some new oxide glasses with many orders of magnitude greater ionic conductivity and dielectric constant than those of the single crystals have been found [1–3]. In the $KNbO_3$–Nb_2O_5 system, many kinds of compounds with various crystal structures [4, 5] have been synthesized and their various physico-chemical properties such as ferroelectric property [6, 7], ionic conductivity [8] and photocatalytic property [9, 10], have been investigated. As mentioned above, the synthesis and investigation of physical and chemical properties of crystalline materials in this system have been carried out. No systematic research on the formation of amorphous materials and their crystallization and electrical properties has been reported. In the present study, various $KNbO_3$–Nb_2O_5 glasses were fabricated by the twin-roller rapidly quenching method and their characteristics were investigated.

2. Experimental procedures

Reagent grade K_2CO_3 and Nb_2O_5 were used as starting materials. These powders were mixed in the desired molar ratio by wet ball-milling using ethyl alcohol, plastic balls and plastic containers for 48 h, and then calcined at 850 °C for 12 h. The calcined powders were uniaxially pressed at 100 MPa to form pellets, 8 mm in diameter and 5 mm in thickness, and placed in a platinum nozzle, 10 mm in diameter and 100 mm in length, supported by alumina tube prior to melting in an electric furnace at 1200 to 1500 °C. After melting was completed, the samples were quenched in the twin-roller of tungsten carbide, 74 mm in diameter and 77 mm in length, rotating at 800 to 2000 r.p.m. and 400 MPa. The quenching rate is estimated as about 10^5 deg sec^{-1} [11]. For comparison, crystalline compounds were also fabricated by sintering the same pellets below the melting temperatures.

The samples were identified by X-ray powder diffractometry using nickel-filtered CuKα radiation. Simultaneous thermogravimetry (TG) and differential thermal analysis (DTA) were carried out at a heating rate of 10 deg min^{-1} to determine the crystallization and melting temperatures. The band gap energy of the product was determined by the onset of ultraviolet–visible absorption spectra. Infrared absorption spectra were measured to examine the coordination state of Nb^{5+} ions in the glasses. Densities were determined by pycnometry. The ionic conductivity and dielectric constant were determined for the glass samples uniaxially pressed at 200 MPa into pellets of 8 mm in diameter and 5 mm in thickness by using YPH LH4192A type impedance analyser in air at 290 to 900 K and frequencies between 5 Hz and 100 kHz in order to prevent the reduction of Nb^{5+} to Nb^{4+}.

0022–2461/91 $03.00 + .12

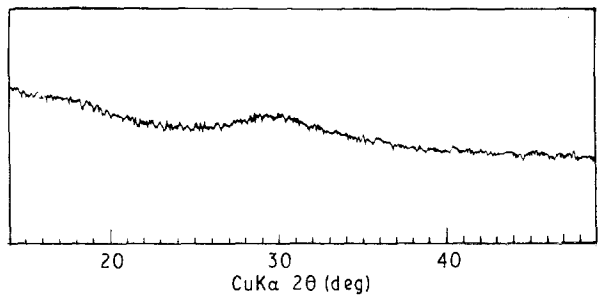

Figure 1 X-ray powder diffraction pattern of quenched $KNbO_3$ sample.

3. Results and discussion

In the present experiments, $KNbO_3$–Nb_2O_5 glasses showing halo patterns in X-ray powder diffraction as shown in Fig. 1 were obtained in the range of molar ratio of K/(K + Nb) from 0.16 to 0.5. The experimental conditions needed to form $KNbO_3$–Nb_2O_5 glasses with representative chemical compositions are summarized in Table I. The quenched samples were ash-coloured opaque flakes, about 7 mm in width, 5 to 100 mm in length and 20 to 70 μm in thickness. The ash-colour of the quenched samples diminished by heating at 400 °C for 1 h.

DTA curves of the $KNbO_3$ glass and $K_2Nb_8O_{21}$ glass are shown in Fig. 2. $KNbO_3$ glass and $K_2Nb_8O_{21}$ glass showed no noticeable endothermic peaks corresponding to the glass transition, but showed sharp exothermic peaks corresponding to the crystallization at 450 and 650 °C, respectively. Since the X-ray powder diffraction patterns of the samples annealed at 500 and 700 °C for 1 h did not agree with those of $KNbO_3$ and $K_2Nb_8O_{21}$ crystals, these glasses seemed to crystallize to stable $KNbO_3$ and $K_2Nb_8O_{21}$ crystals via metastable phases. The broad exothermic peaks observed at 700 to 800 °C and 700 to 850 °C, respectively, might be attributed to the phase transformation of these metastable phases to stable phases. The crystallization temperatures and the phase transformation sequences of the glasses in the $KNbO_3$–Nb_2O_5 system are shown in Fig. 3. The reaction phase diagram of the $KNbO_3$–Nb_2O_5 system constructed by the TG-DTA and XRD analyses of the calcined samples is also shown in Fig. 3. Seven compounds such as $KNbO_3$, $K_4Nb_6O_{17}$, $K_2Nb_4O_{11}$, $K_3Nb_7O_{19}$, KNb_3O_8, $K_2Nb_8O_{21}$ and Nb_2O_5 were formed by the calcination in the present experimental conditions. These results agreed with those reported by Lundberg and Sundberg [5]. As seen in Fig. 3, the

TABLE I Experimental conditions to prepare some $KNbO_3$–Nb_2O_5 glasses

Composition	Melt temperature (°C)	Rotation speed of rollers (r.p.m.)
$KNbO_3$	1300	1000
$K_4Nb_6O_{17}$	1350	950
$K_2Nb_4O_{11}$	1450	1200
$K_3Nb_7O_{19}$	1450	1200
KNb_3O_8	1400	975
$K_2Nb_8O_{21}$	1550	975

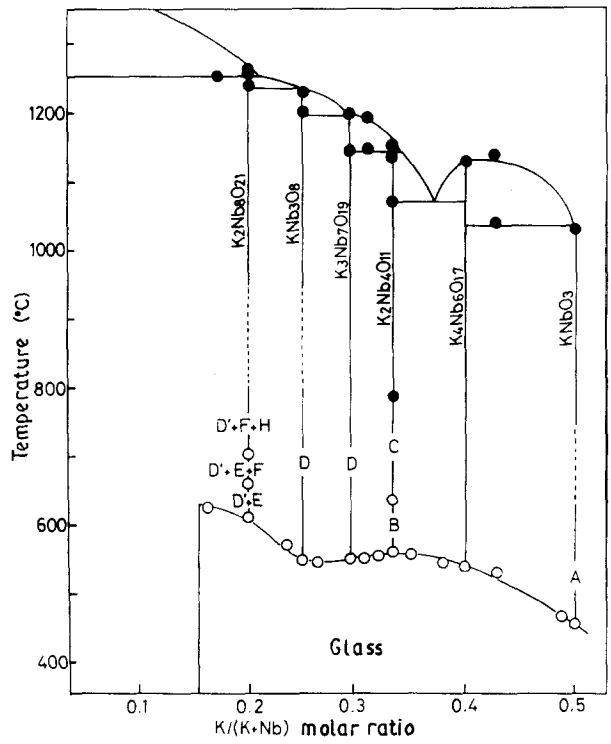

Figure 2 DTA curves of $KNbO_3$ glass (A) and $K_2Nb_8O_{21}$ glass (B). (● endotherm, ○ exotherm, ---- broad transition)

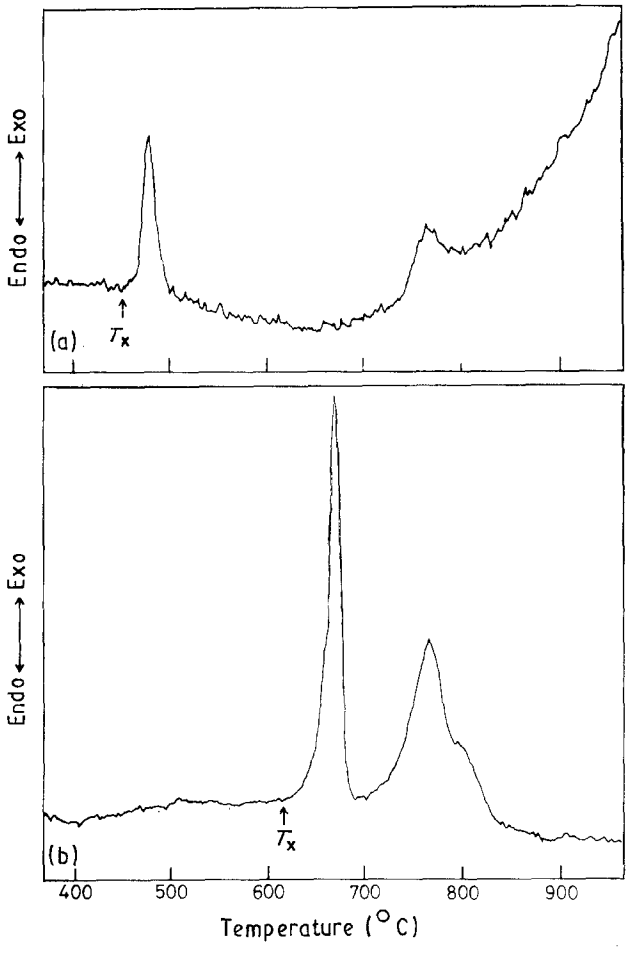

Figure 3 Crystallization temperature, phase transformation sequence of the glasses and reaction phase diagram in the $KNbO_3$–Nb_2O_5 system.

TABLE II X-ray powder diffraction data of the metastable phases of A to H

A phase		B phase		C phase		D phase		E phase		F phase		H phase	
d (nm)	Intensity	*d* (nm)	Intensity	*d* (nm)	Intensity	*d* (nm)	Intensity	*d* (nm)	Intensity	*d* (nm)	Intensity	*d* (nm)	Intensity
0.787	m	0.616	m	0.550	m	0.792	vw	0.655	m	0.1077	m	0.842	vs
0.737	vs	0.584	w	0.3882	vs	0.603	m	0.3871	m	0.3422	vs	0.514	vw
0.700	s	0.523	m	0.3663	vw	0.522	vw	0.3254	vs	0.3151	m	0.503	vw
0.394	vw	0.3072	vs	0.2091	w	0.4282	w	0.2848	m	0.2809	w	0.4213	w
0.3606	vw	0.3047	vs	0.2078	w	0.3967	m	0.1880	vw			0.3811	m
0.3331	vs	0.2875	vw			0.3647	m	0.1863	vw			0.3741	m
0.3188	vs	0.2800	vs			0.3312	m	0.1627	m			0.3538	w
0.3144	vs	0.2655	vw			0.3076	vw					0.3220	vs
0.2992	m	0.2610	vw			0.3015	vs					0.2543	vw
0.2828	m	0.2496	w			0.2909	m					0.2460	w
0.2620	w	0.2194	vw			0.2809	w					0.2422	w
0.2519	w	0.2051	w			0.2083	vw					0.2088	w
0.2471	vw	0.1983	vw			0.2644	vw					0.2038	vw
0.2386	m	0.1939	w			0.2359	vw					0.2013	vw
0.2226	vw	0.1879	w			0.2293	vw					0.1950	vw
0.2129	m	0.1814	m			0.2281	vw					0.1847	vw
0.2052	m	0.1762	vw			0.2171	vw					0.1741	m
		0.1718	w			0.2108	vw					0.1711	vw
		0.1670	vw			0.1984	vw						
		0.1605	vw			0.1970	vw						
		0.1542	m			0.1952	vw						
						0.1888	vw						
						0.1852	vw						
						0.1841	vw						
						0.1824	vw						
						0.1805	vw						
						0.1755	vw						
						0.1767	vw						
						0.1759	vw						
						0.1705	m						
						0.1624	vw						

s: strong, m: medium, w: weak, v: very.

crystallization temperature of the glasses showed similar compositional dependence to liquidus curve in the reaction phase diagram. Only $K_4Nb_6O_{17}$ glass directly crystallized to $K_4Nb_6O_{17}$ crystal, but the crystallization of other glasses proceeded via metastable phases. The X-ray powder diffraction patterns of the metastable phases are summarized in Table II. The identification of the crystalline structures of these metastable phases is now in progress.

The band gap energies of $KNbO_3$–Nb_2O_5 glasses and polycrystals determined by the onset of the ultraviolet–visible absorption spectra are shown in Fig. 4. The band gap energies of the polycrystals were in the range of 3.1 to 3.6 eV, and changed discontinuously with the composition. On the other hand, the band gap energies of the glasses increased from 3.3 to 3.9 eV with increasing K/(K + Nb) molar ratio from 0.16 to 0.5. The values of the band gap energies were slightly higher than those of the polycrystals. These results indicated that the glass structures changed continuously with increasing K^+ ion content.

Infrared absorption spectra of the $KNbO_3$ polycrystals and various $KNbO_3$–Nb_2O_5 glasses are shown in Fig. 5. The $KNbO_3$ crystal showed a sharp absorption peak at 620 cm^{-1} corresponding to Nb–O stretching of the corner-shared NbO_6 octahedra [12]. The considerable broadening of the peaks around 620 cm^{-1} in the glass samples might be interpreted by symmetry lowering. Other broad peaks attributed to the stretching of Nb–O in the edge-shared NbO_6 octahedra [12] were observed around 900 cm^{-1} in the glass samples except for $KNbO_3$ glass. The intensity of the peak around 900 cm^{-1} increased with decreasing K^+ ion content. These results indicated that $KNbO_3$ glass structure consisted of the corner-shared NbO_6 octahedra, and the number of the edge-shared NbO_6 octahedra increased with decreasing K^+ ion content.

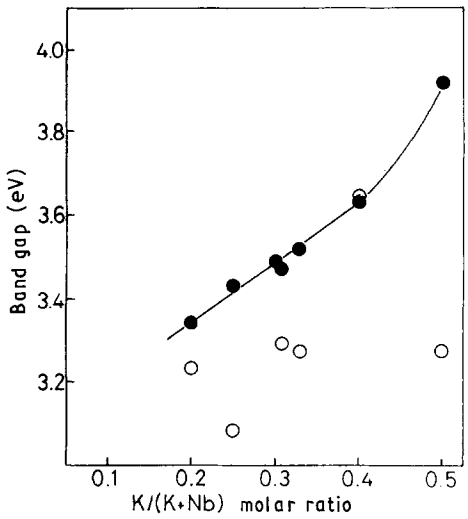

Figure 4 Optical band gap of $KNbO_3$ glasses and crystals.

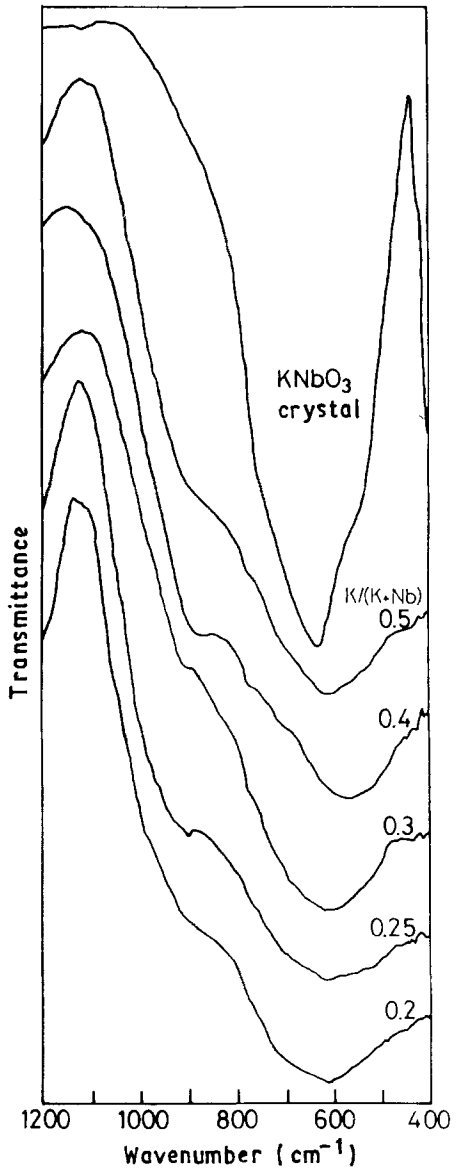

Figure 5 Infrared spectra of $KNbO_3$–Nb_2O_5 glasses and $KNbO_3$ crystal. The molar ratio of K/(K + Nb) of 0.5, 0.4, 0.3, 0.25 and 0.2 refer to $KNbO_3$ glass, $K_4Nb_6O_{17}$ glass, $K_3Nb_7O_{19}$ glass, KNb_3O_8 glass and $K_2Nb_8O_{21}$ glass, respectively.

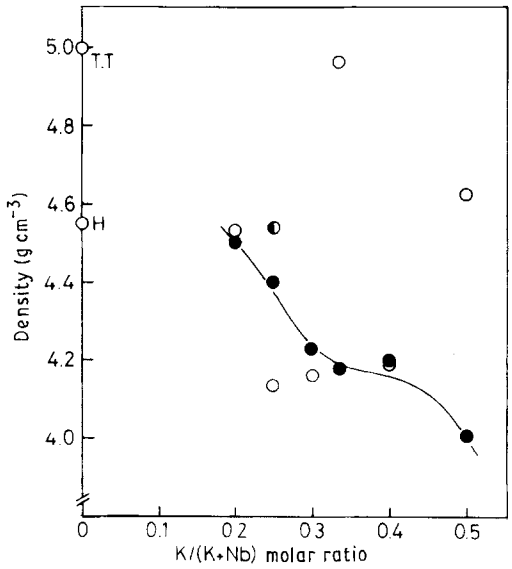

Figure 6 Measured densities of $KNbO_3$–Nb_2O_5 glasses (●) and metastable phase (◐) and theoretical densities (○) of $KNbO_3$–Nb_2O_5 compounds as a function of the K/(K + Nb) molar ratio.

Compositional dependence of the density of the glass samples is shown in Fig. 6 together with the theoretical densities of the crystals. The theoretical densities of the crystals changed discontinuously with the compositional change. It is seen that the theoretical densities of the layer structure compounds such as $K_4Nb_6O_{17}$ and KNb_3O_8 and the tunnel structure compound of $K_3Nb_7O_{19}$ are much smaller than others. On the other hand, the densities of the glasses decreased continuously with increasing K^+ ion content. These results indicated that the Nb–Nb distance in the glasses decreased with decreasing K^+ ion content due to increasing the amount of edge shared by NbO_6 octahedra. It is well known that the density of glass is smaller than that of the crystalline sample. In the present study, as seen in Fig. 6, the density of glass is larger than that of the crystalline sample with layer and tunnel structures. For the sample with chemical composition of KNb_3O_8, the density of the crystalline sample with layer structure is much smaller than that of glass sample, but the density of metastable phase is larger than that of glass. The detailed discussion is not clarified at the present time, but the present results will give us interesting information on the relationship between glass structure and crystal structure. $KNbO_3$–Nb_2O_5 compounds are expected to possess K^+ ion ionic conductivity. The a.c. electrical conductivity, σ, of $KNbO_3$–Nb_2O_5 compounds was measured at frequencies between 5 Hz and 100 kHz at 290 to 900 K in air. It is well known that the reduction of Nb^{5+} to Nb^{4+} occurs at a high temperature in an inert gas atmosphere and in vacuum, but this was not observed in the present experimental conditions. The plots of $\ln(\sigma T)$ against T^{-1} for the various $KNbO_3$–Nb_2O_5 glasses are shown in Fig. 7, where T_x indicates the crystallization temperature of the glass. As expected for the ionic conduction, in each experiment the plot was a straight line up to a temperature of 100 K lower than the crystallization temperature, therefore, it could be suspected that the glass transition or the nucleation reaction of the glasses started at a temperature of 100 K lower than the crystallization temperature. The activation energies determined from the slopes of the straight lines and the electric conductivities at 300 °C are plotted as a function of the molar ratio of K/(K + Nb) in Fig. 8 together with those of the polycrystals. The activation energies of the glasses and the crystals were 65 to 85 kJ mol^{-1}, which seemed to be adequate for K^+ ion ionic conduction. Although the activation energies and electric conductivities of the crystals changed discontinuously with the composition, the increment of K^+ ion content in the glasses resulted in the decrease of the activation energy and the increase in the electric conductivity. The increase in the electric conductivity might be interpreted by the increase in the carrier concentration. On the other hand, the decrease in the activation energy might be due to the decrease in the energy barrier to migrate K^+ ion in the channel with increasing the number of corner-shared NbO_6 octahedra.

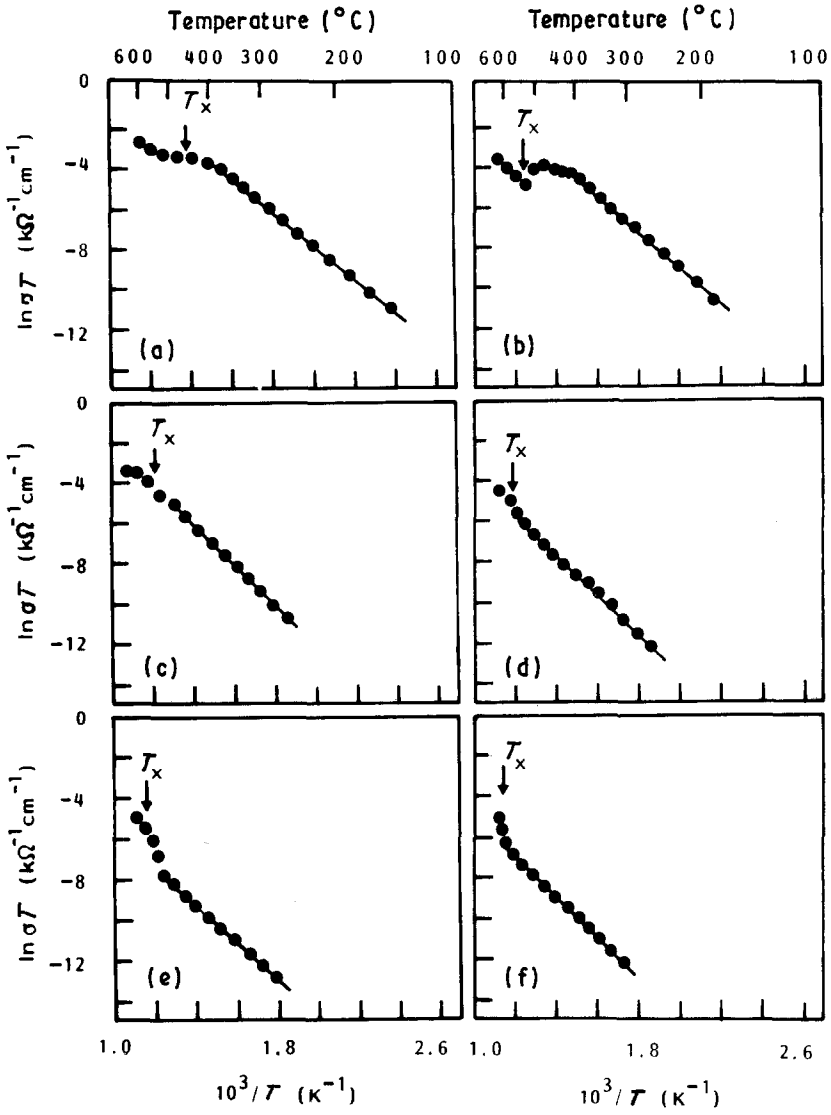

Figure 7 Plots of $\ln \sigma T$ against $1/T$ for $KNbO_3$–Nb_2O_5 glasses. (a) $KNbO_3$, (b) $K_4Nb_6O_{17}$, (c) $K_2Nb_4O_{11}$, (d) $K_3Nb_7O_{19}$, (e) KNb_3O_8, (f) $K_2Nb_8O_{21}$.

The temperature dependence of the dielectric constants of $KNbO_3$ polycrystals and $KNbO_3$ glasses at the frequencies of 1, 10 and 100 kHz are shown in Fig. 9. The peaks at 210 and 415 °C observed for the dielectric constants of ferroelectric $KNbO_3$ polycrystals were attributed to the orthorhombic to tetragonal and the tetragonal to cubic phase transformations, respectively. Although it is reported that the dielectric constants of $LiNbO_3$ glass were many orders of magnitude larger than those of $LiNbO_3$ crystal [1, 2], the dielectric constants of the $KNbO_3$ glass were much smaller than those of the $KNbO_3$ polycrystals around room temperature. The dielectric constants of the $KNbO_3$ glass increased with increasing temperature, but the temperature coefficient of the dielectric constants was small at high frequency. The dielectric constants of the $KNbO_3$ glass around the crystallization temperature approached those of $KNbO_3$ polycrystals at 1 kHz, but were much lower than those of polycrystals at high frequencies such as 10 and 100 kHz. These results indicated that the ferroelectric property of the $KNbO_3$ glass might be interpreted by space-charge polarization [13].

The temperature dependence of the dielectric constants of various $KNbO_3$–Nb_2O_5 glasses is shown in Fig. 10. As seen in Fig. 10, the dielectric constants at low temperature increased with decreasing K^+ ion concentration. The magnitude of the dielectric constant at 25 °C was in the order of $K_2Nb_8O_{21} > KNb_3O_8 = K_3Nb_7O_{19} = K_2Nb_4O_{11} > K_4Nb_6O_{17} > KNbO_3$. These results might be interpreted by a symmetry lowering in the glass structure due to increasing number of edge-shared NbO_6 octahedra. On the other hand, since the temperature coefficient of the dielectric constants increased with increasing K^+ ion content, the dielectric constants increased with increasing K^+ ion content, the dielectric constant at 400 °C was in the order of $KNbO_3 > K_4Nb_6O_{17} > K_2Nb_4O_{11} = K_3Nb_7O_{19} > KNb_3O_8 = K_2Nb_8O_{21}$. These results indicated that the dielectric constants of the $KNbO_3$–Nb_2O_5 glasses were predominantly affected by space-charge polarization at high temperature.

4. Conclusions

The conclusions are as follows.

(1) $KNbO_3$–Nb_2O_5 glasses were prepared in the range of the molar ratio of K/(K + Nb) from 0.16 to 0.5 by the twin-roller rapidly quenching method.

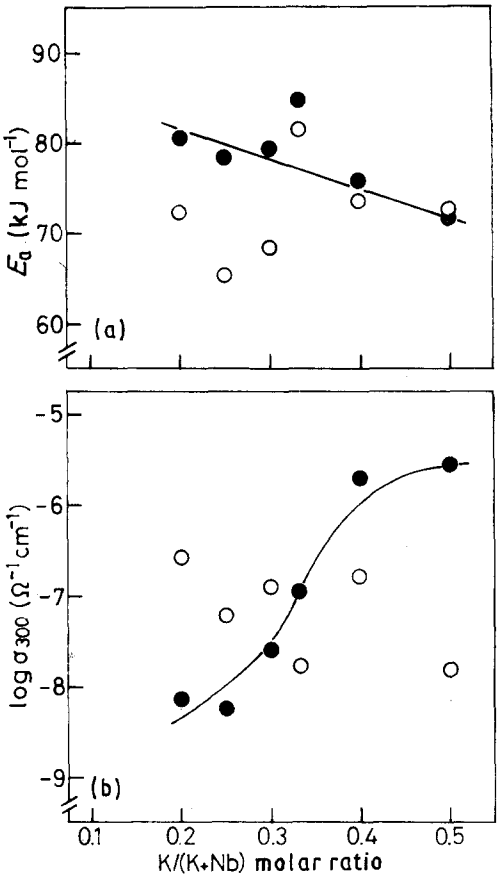

Figure 8 (a) Activation energy and (b) electrical conductivity at 300 °C of the $KNbO_3$–Nb_2O_5 glasses and polycrystals as a function of the K/(K + Nb) molar ratio.

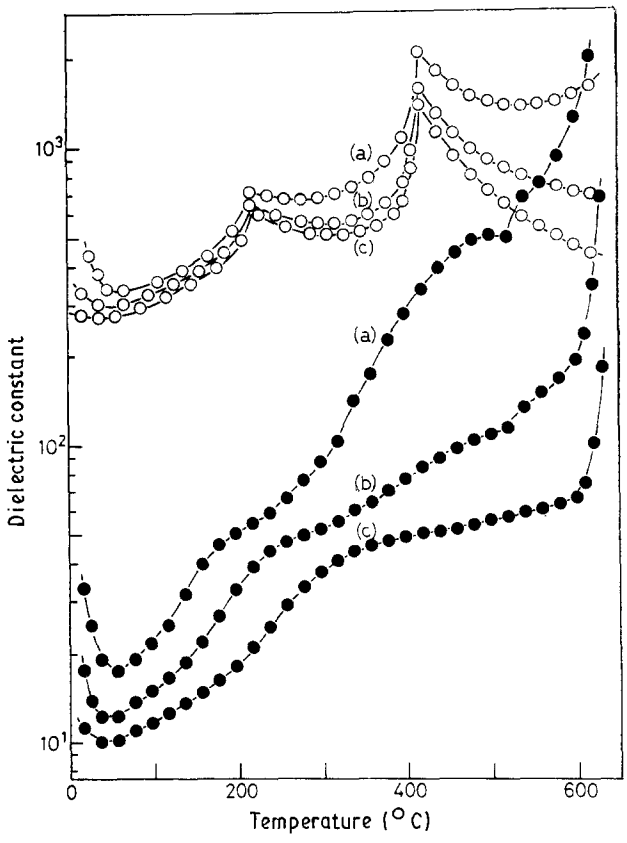

Figure 9 Temperature dependence of the dielectric constants of $KNbO_3$ polycrystals (○) and $KNbO_3$ glasses (●) at a frequency of (a) 1 kHz, (b) 10 kHz and (c) 100 kHz.

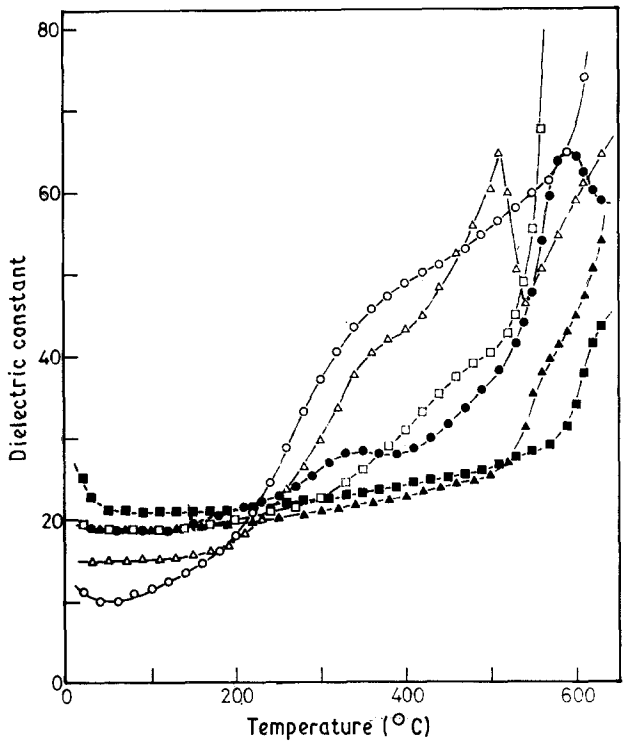

Figure 10 Temperature dependence of the dielectric constants of $KNbO_3$–Nb_2O_5 glasses at 100 kHz. $KNbO_3$ glass (○), $K_4Nb_6O_{17}$ glass (△), $K_2Nb_4O_{11}$ glass (□), $K_3Nb_7O_{19}$ glass (●), KNb_3O_8 glass (▲), $K_2Nb_8O_{21}$ glass (■).

(2) $K_4Nb_6O_{17}$ glass directly crystallized to $K_4Nb_6O_{17}$ crystals, but the crystallization of other glasses proceeded via metastable phases.

(3) $KNbO_3$ glass consisted of corner-shared NbO_6 octahedra, but the number of edge-shared NbO_6 octahedra increased with decreasing K^+ ion content.

(4) The band gap energy and the ionic conductivity of the $KNbO_3$–Nb_2O_5 glasses increased with increasing K^+ ion content, but the density and the activation energy of ionic conduction decreased.

(5) $KNbO_3$ glass possessed high dielectric constants approaching ferroelectric $KNbO_3$ crystals at high temperature and low frequency, but the dielectric constants of the $KNbO_3$ glass decreased with decreasing temperature and increasing frequency.

(6) The dielectric constants of the $KNbO_3$–Nb_2O_5 glasses at low temperature decreased with increasing K^+ ion content, but those at high temperature increased.

References

1. A. M. GLASS, M. E. LINES, K. NASSAU and J. W. SHIEVER, *Appl. Phys. Lett.* **31** (1977) 249.
2. A. M. GLASS, K. NASSAU and T. J. NEGRAN, *J. Appl. Phys.* **49** (1978) 4808.
3. H. L. TULLER, D. P. BUTTON and D. R. UHLMANN, *J. Non-cryst. Solids* **40** (1980) 93.
4. K. NASSAU, C. A. WANG and M. GRASSO, *J. Amer. Ceram. Soc.* **60** (1979) 74.
5. M. LUNDBERG and M. SUNDBERG, *J. Solid State Chem.* **63** (1986) 216.
6. K. NASSAU, J. W. SHIEVER and J. L. BERNSTEIN, *J. Electrochem. Soc.* **116** (1969) 348.
7. A. M. QUITTET, J. L. SERVOIN and F. GERVAIS, *J. Physique* **42** (1981) 493.

8. J. SINGER, W. L. FIELDER, H. E. KAUTZ and J. S. FORDYCE, *J. Electrochem. Soc.* **123** (1976) 614.
9. K. DOMEN, A. KUDO, A. SHINOZAKI, A. TANAKA, K. MARUYA and T. ONISHI, *J. Chem. Soc., Chem. Commun.* (1986) 356.
10. F. D. QUARTO, S. PIAZZA, R. D'AGOSTINO and C. SUNSERI, *J. Electroanal. Chem.* **228** (1987) 119.
11. K. NASSAU, C. A. WANG and M. GRASSO, *J. Amer. Ceram. Soc.* **62** (1979) 74.
12. M. TATSUMISAGO, A. HAMADA, T. MINAMI and M. TANAKA, *J. Amer. Chem. Soc.* **66** (1983) 118.
13. M. S. MIZZONI, *J. Electrochem. Soc.* **120** (1973) 1502.

Received 31 July 1989
and accepted 19 February 1990